Journal of Non-Crystalline Solids 357 (2011) 829–835

Contents lists available at ScienceDirect

Journal of Non-Crystalline Solids

journal homepage: www.elsevier.com/ locate/ jnoncrysol

Conversion of batch to molten glass, I: Volume expansion

Samuel H. Henager, Pavel Hrma *, Kevin J. Swearingen, Michael J. Schweiger, José Marcial, Nathan E. TeGrotenhuis

Pacific Northwest National Laboratory, Richland, WA 99354, United States

ARTICLE INFO

Article history:
Received 17 September 2010
Received in revised form 13 November 2010
Available online 20 December 2010

Keywords:
Glass formation;
Foam;
Silica;
Sucrose;
Melting

ABSTRACT

Batches designed to simulate nuclear high-level waste glass were compressed into pellets that were heated at 5 K/min and photographed. Three types of batches were prepared, each with different amounts of nitrates and carbonates. The all-nitrate batches were prepared with varying amounts of sucrose. The mixed nitrate–carbonate batches were prepared with silica particles ranging in size from 5 to 195 μm. One batch containing only carbonates was also tested. Sucrose addition had little effect on expansion, while the size of silica was very influential. Sucrose addition reduced primary foam for batches containing 5-μm silica, but had no effect on batches containing larger particles. Excessive amounts of sucrose increased secondary foam. The 5-μm grains had the strongest effect, causing both primary and secondary foam to be generated, whereas only secondary foam was produced in batches with grains of 45 μm and larger. We suggest that the viscosity of the melt and the amount of gas evolved are the main influences on foam production. As more gas is produced in the melt and as the glass becomes less viscous, gas bubbles coalesce into larger cavities until the glass can no longer contain the bubbles and they burst, causing the foam to collapse.

1. Introduction

1.1. Background and purpose

This study is concerned with the effect of silica grain size and exothermic reactions on batch expansion caused by foam generation. Apart from glass-foam production, foaming is considered an undesirable phenomenon in glass making because it insulates the unmelted batch from the heat flow from molten glass and thus slows down the rate of melting [1,2]. Two types of foam have been distinguished by Gerrard and Smith [3]: primary foam within the glass batch itself and secondary foam within the molten glass, the former being produced by gases from batch reactions and the latter by gases from oxidation–reduction reactions or other fining gases. The subject of this paper is foaming in batches designed to simulate nuclear high-level waste (HLW) glass. Though the composition of nuclear waste glasses varies considerably, only one glass composition was selected for this study (see Section 2.1).

As we stressed in previous papers [4–7], the impact of primary foam on the batch melting process is not entirely clear, though it appears to have a generally negative effect. While primary foam does help homogenize the melt and assists in the dissolution of residual solids, batches that strongly foam have been shown to melt slower than batches producing limited foam [8]. Secondary foam has an especially negative effect on glass processing. Fortunately, this effect can be limited or avoided by bubbling air through the melt [9].

As in the previous studies [4–8], our main concern is to gain knowledge of how to influence batch expansion by changing the batch makeup without changing the glass composition. In the case of waste glass, these changes are limited to adjusting the glass-forming and modifying additives because the waste is processed as received. The usefulness of the data presented is twofold: first, the results will help adjust the batch makeup to control foaming if needed; and second, the data will be used in a mathematical model of the cold cap in the waste-glass melter.

In this study, we examine the effects of quartz particle size and the reaction between sucrose and nitrates on the volume expansion during melting of HLW batches. Sucrose has been added in the past because its reaction with nitrates generates heat that can enhance the rate of melting. Our purpose was to examine whether sucrose addition would impact foaming during the melting process. We prepared 11 batches, all designed to make a high-alumina HLW glass. These batches can be divided into three groups: A0-AN1, A0-AN2, and A0-AC. These batches were also compared to A0 batches from an earlier study [6].

All batches contained metallic oxides and hydroxides as well as varying amounts of carbonates and nitrates. The A0 group comprised three batches with nitrates and carbonates. The individual batches were made with 5-, 75-, and 195-μm particles of quartz. No sucrose was added to these batches. The A0-AN1 group comprised five batches containing primarily nitrates, though carbonates were used to simulate some waste components. The individual batches were made with 5-, 45-, 75-, 150-,

* Corresponding author.
E-mail address: pavel.hrma@pnl.gov (P. Hrma).

0022-3093/$ – see front matter © 2010 Elsevier B.V. All rights reserved.
doi:10.1016/j.jnoncrysol.2010.11.102

and 195-μm quartz particles. Sucrose was added to batches so that the carbon-to-nitrogen molar ratio (C/N) was equal to 1. The A0-AN2 group comprised five batches containing nitrates and no carbonates. All A0-AN2 batches were made with 75-μm quartz particles. Varying amounts of sucrose were added to the five batches so that C/N = 0.00, 0.50, 0.75, 1.00, and 1.25, respectively. The A0-AC group comprised one batch containing carbonates and no nitrates. No sucrose was added. The quartz particle size for this batch was also 75 μm.

Batches were prepared as slurries to simulate actual melter batches. In preparation for testing, batches were dried and pressed into cylindrical pellets approximately 6 mm high and 13 mm in diameter. Pellets were heated at 5 K/min from room temperature to 1000 °C. Pellets were chosen over silica-glass crucibles to avoid bridging and obtain more accurate measurements.

1.2. A note on terminology

It should be noted that the mixture of glass precursors is called a "batch" in this paper as a concession to the traditional terminology from the times before continuous glass melting was developed. In the waste-glass community, the term "feed" is preferred because the material is charged, or "fed," to the melter in the form of water slurry. However, the term "batch" is not entirely inappropriate for waste-glass making because the feed is prepared by mixing the ingredients in batches that are only later charged continuously into the waste-glass melter. Therefore, we use the term "batch" in this paper to be consistent with the literature on glass technology.

2. Experimental

2.1. Composition of batches

Table 1 lists the compositions of the batches tested. All batches were formulated to make a high-alumina HLW glass. The glass was designed to contain 45 mass% waste simulants and 55 mass% glass-forming additives. The glass components and their mass fractions are SiO_2 (0.305), Al_2O_3 (0.240), B_2O_3 (0.152), Na_2O (0.096), CaO (0.061), Fe_2O_3 (0.059), Li_2O (0.036), Bi_2O_3 (0.011), P_2O_5 (0.011), F (0.007), Cr_2O_3 (0.005), PbO (0.004), NiO (0.004), ZrO_2 (0.004), SO_3 (0.002), K_2O (0.001), MgO (0.001), and ZnO (0.001).

Table 1
Batch compositions (in g) to make 1 kg of glass.

	Batch Composition (g/kg of glass)			
Compound	A0	A0-AC	A0-AN1	A0-AN2
$Al(OH)_3$	367.49	367.49	367.49	367.49
$B(OH)_3$	269.83	269.83	269.83	269.83
$Bi(OH)_3$	12.80	12.80	12.80	12.80
$CaCO_3$	0.00	108.49	0.00	0.00
$Ca(NO_3)_2{\cdot}4H_2O$	0.00	0.00	210.56	210.56
CaO	60.79	0.00	10.79	10.79
$Fe(H_2PO_2)_3$	12.42	12.42	12.42	12.42
$Fe(OH)_3$	73.82	73.82	73.82	73.82
K_2CO_3	0.00	2.08	0.00	0.00
KNO_3	3.04	0.00	3.04	3.04
Li_2CO_3	88.30	88.30	4.22	0.00
$LiNO_3$	0.00	0.00	156.90	164.78
$Mg(OH)_2$	1.69	1.69	1.69	1.69
NaF	14.78	14.78	14.78	14.78
$NaNO_2$	3.37	3.37	3.37	3.37
$NaNO_3$	4.93	12.34	112.97	112.97
NaOH	97.14	16.22	46.30	46.30
Na_2CO_3	0.00	102.60	0.00	0.00
$Na_2C_2O_4$	1.76	1.26	1.26	1.26
Na_2CrO_4	11.13	11.13	11.13	11.13
Na_2SO_4	3.55	3.55	3.55	3.55
$NiCO_3$	6.36	6.36	6.36	0.00
$Ni(NO_3)_2{\cdot}6H_2O$	0.00	0.00	0.00	15.58
$PbCO_3$	0.00	4.91	0.00	0.00
$Pb(NO_3)_2$	6.08	0.00	6.08	6.08
SiO_2	305.05	305.05	305.05	305.05
$Zn(NO_3)_2{\cdot}4H_2O$	2.67	0.00	2.67	2.67
ZnO	0.00	0.83	0.00	0.00
$Zr(OH)_4{\cdot}xH_2O$	5.11	5.49	5.49	5.49
Totals	1352.10	1424.80	1642.57	1655.43

The batches listed in Table 1 differ in the fractions of volatile anionic portions of salts. The baseline batch, A0, contains hydroxides, nitrates, and carbonates. This batch was prepared and tested previously [6]; it is included in this study for completeness. In the A0-AN1 batch, the content of carbonates is limited to waste components. No carbonates are present in the A0-AN2 batch. Finally, the A0-AC batch contains carbonates and no nitrates. Reagent grade chemicals were used to make batches.

2.2. Preparation of batches

Batch slurries, either 500 or 1000 ml in volume, were wet-mixed. Approximately 2 ml of deionized H_2O was used per gram of batch. The volume of slurry was 0.5 or 1 l. The water was heated to 60 to 80 °C and stirred with an impeller while adding all chemicals except quartz. Water-soluble components were added first and then the oxides, hydroxides, and oxyhydrates of heavy metals, and finally sucrose (if necessary). Silica was added in the form of crushed quartz after all other components (see Section 2.4).

This method was selected because it crudely mimics the nature of the HLW while still being easy to carry out. It is a simplified version of more complex methods that involve co-precipitating the various hydroxides from their respective nitrates using sodium hydroxide [10].

2.3. Addition of sucrose

After all the glass compounds had been mixed, sucrose was added. The sucrose was added based on the calculated amount of nitrogen (in the form of nitrates and nitrites) contained in the batch. For the A0-AN1 batch, sucrose was added in a 1:1 carbon-to-nitrogen molar ratio; i.e., C/N = 1. For the A0-AN2 batch, five batches were prepared, one with no sucrose and then four more with C/N = 0.50, 0.75, 1.00, and 1.25. The mass fraction of sucrose in each batch was 0.05, 0.07, 0.09, and 0.11, respectively. Sucrose was added as the final component before a batch was dried. For batches with varying amounts of sucrose, the C/N ratio is added in parentheses at the end of the batch label, e.g., A0-AN2 (0.50).

The batch slurry was carefully dried over a hot plate and under a heat lamp to drive off most of the water. After most of the water had evaporated, the batch was transferred to a stainless steel container where it was further dried. An impeller was used to keep mixing the batch throughout this process. Once the batch became too viscous for the impeller, it was mixed with a large putty knife. After it had fully dried, the batch was crushed to a powder before being dried overnight in an oven at 105 °C. Finally, the batch was crushed and homogenized in a tungsten carbide mill.

2.4. Selection of silica grains and completion of batch preparation

The A0 batches were tested with 5-, 75-, and 195-μm particles of quartz and the A0-AN1 batches 5-, 45-, 75-, 150-, and 195-μm particles. The following sources of quartz were used: US Silica MIN-U-SIL® 5, SIL-CO-SIL® 45, and SIL-CO-SIL® 75 for 5-, 45-, and 75-μm particles, Lane Mountain for 150-μm particles, and Aldrich for 195-μm particles. The number at the end of A0 and A0-AN1 batch labels (e.g., A0-AN1-75) denotes the particle size of the quartz used. In A0-AC and A0-AN2 batches, only 75-μm quartz particles were used.

To ensure the correct fraction of silica in each sample, quartz was added separately from the other components. This fraction was determined using loss on ignition (LOI) tests. Four 5-g batches were prepared that contained approximately 20 mass% 75-μm crushed quartz. The masses of the samples were recorded, the samples were

heated in porcelain crucibles for 1 h at 1050 °C, and the final masses were recorded. The difference in mass between the batch weight and glass weight was used to determine the correct percent of silica required in the batch to obtain glass that contained 30.51 mass% silica. The required mass fraction of quartz in a batch is given by $f_g m_g/m_b$, where f_g is the desired fraction of silica in the glass (in this case 0.3051), m_g is the mass of glass produced during the LOI test, and m_b is the initial mass of the batch and quartz prepared for the LOI test. Once the correct fraction of quartz was determined, quartz was mixed with the batch in an agate mill. Only as much batch as was needed for a test was prepared at any time.

2.5. Making and heating pellets

Batch samples were pressed into 1.5-g pellets at ~7 MPa. The loose batch was poured into a pellet press mold and brought to 7 MPa for 10 s. Then the pressure was released for 10 s, reapplied for 10 s, released for 10 s, and then applied for 180 s, after which the pellet was ready for heat treatments.

For each test, a pellet was placed on a small alumina plate in a windowed furnace. Starting from room temperature, the furnace was heated at 5 K/min to a final temperature of 1000 °C where it was held for 1 h. Alongside the pellet in the furnace was a 10-mm-long section of platinum wire (seen at the right edge of each picture in Figs. 1 and 2). Pictures were taken of the pellet every 50 °C to 200 °C, after which pictures were taken every 25 °C. At least two pellets from each batch (except batches A0-75 and A0-195) were tested. Fig. 1 shows various shapes a pellet underwent during a heat treatment.

2.6. Developing and evaluating the batch expansion curves and porosity

The pictures were evaluated using Adobe Photoshop CS3 Extended (v. 10.0.1). The platinum wire was used as a scale gauge, which allowed the program to calculate the area of the cross section of the pellet (A) as displayed in the picture. Each pellet was measured twice to ensure accuracy. The measured area was normalized to the calculated profile area of a hemisphere that the bubble-free glass would occupy. The hemispherical area is given by

$$A_g = \frac{1}{2}\left(\frac{9}{4}\pi\right)^{\frac{1}{3}}\left(\frac{m_f f}{\rho_g}\right)^{\frac{2}{3}} \quad (1)$$

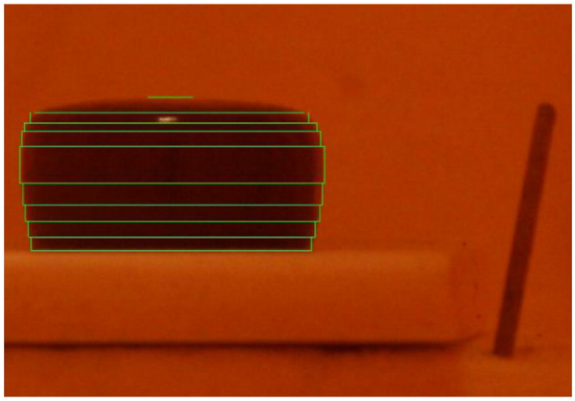

Fig. 2. An A0-AN2 (1.25) pellet at 850 °C. The green lines indicate the cylindrical sections and spherical cap used to approximate the volume of this pellet.

where m_f is the mass of the pellet, f is the ratio of the mass of glass to the mass of the batch, and ρ_g is the density of the glass, approximately 2.6 g/ml.

To determine the relative volume and porosity, the approximate volume of the pellet (V) was determined from its profile and compared to the actual volume of glass (V_g) as calculated from the mass of each pellet. Volumes were obtained for A0-AN2 (0.00), A0-AN2 (0.50), and A0-AN2 (0.75) from 825 °C to 925 °C and for A0-AN2 (1.00) and A0-AN2 (1.25) from 800 °C to 925 °C. At 800 °C and 825 °C, pellets retained their original cylindrical shape, and their volumes were calculated as such. At 900 °C and 925 °C, the pellet volumes were approximated as spherical caps. Otherwise, the profiles of pellets were divided into 4 to 9 cylindrical layers stacked on top of each other covered with a spherical cap, as shown in Fig. 2. The volume of each pellet was obtained as a sum of volumes of the cylindrical disks and the spherical cap.

3. Results

Results pertinent to expansion of batches are summarized in Table 2.

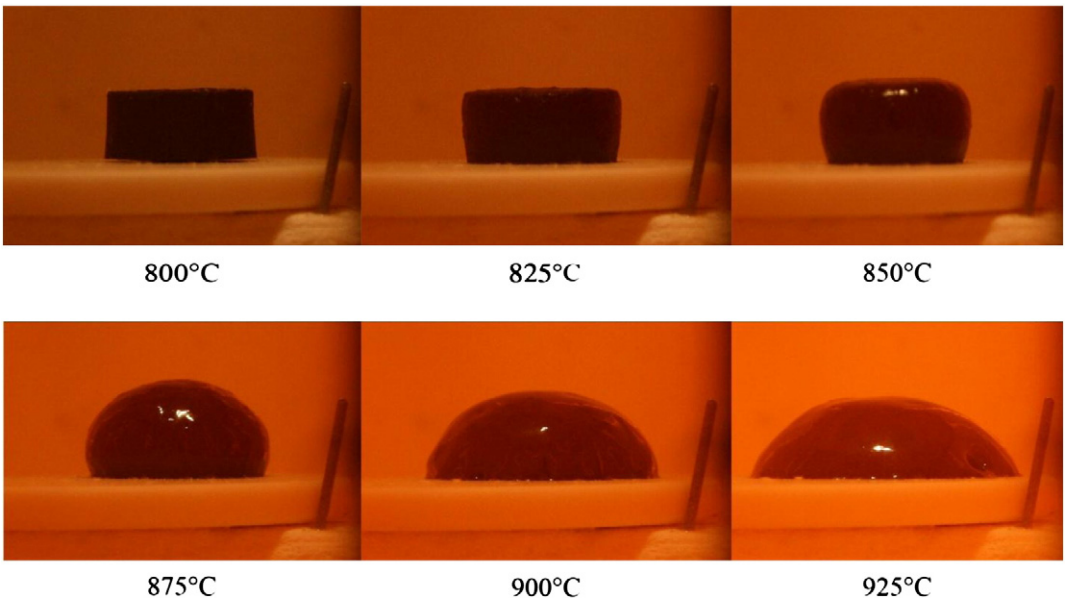

Fig. 1. Pictures of an A0-AN2 (1.00) pellet during a heat treatment. The length of the Pt wire seen to the right of each pellet is 10 mm.

Table 2
All batches along with their temperatures of minimum and maximum expansions (T_{min} and T_{max}) and minimum and maximum areas (A_{min}/A_g and A_{max}/A_g). For A0-AN2 batches only, minimum and maximum volumes (V_{min}/V_g and V_{max}/V_g) are also given.

Batch	Quartz particle size (μm)	T_{min} (°C)	A_{min}/A_g	V_{min}/V_g	T_{max} (°C)	A_{max}/A_g	V_{max}/V_g
A0-5	5	600	1.41		835	4.15	
A0-75	75	840	1.22		880	1.38	
A0-195	195	875	1.21		900	1.34	
A0-AC	75	825	0.90		875	0.99	
A0-AN1-5	5	775	1.35		856	2.66	
A0-AN1-45	45	800	1.01		880	1.49	
A0-AN1-75	75	825	1.17		875	1.61	
A0-AN1-150	150	880	1.04		900	1.11	
A0-AN1-195	195	880	0.98		900	1.05	
A0-AN2 (0.00)	75	825	0.86	0.97	925	1.43	7.82
A0-AN2 (0.50)	75	825	0.90	1.05	925	1.40	8.01
A0-AN2 (0.75)	75	825	0.88	1.01	925	1.43	7.94
A0-AN2 (1.00)	75	800	1.18	1.48	925	1.94	10.91
A0-AN2 (1.25)	75	800	1.19	1.35	925	2.04	10.23

3.1. A0 batch

Expansion of the A0 batches is detailed in a previous paper [6]. Fig. 3 shows the average relative pellet area, A/A_g, versus temperature, where A is the measured pellet profile area and A_g is the calculated hemispherical area as defined in Eq. (1). The error bars indicate the standard deviations based on the tests for each batch. Batches A0-75 and A0-195 do not have error bars as only one pellet was tested for these batches (see Table 2).

3.2. A0-AN1

Fig. 4 Shows A/A_g versus temperature for the A0-AN1 batches. These batches followed a similar trend as the A0 batches [6], though on a smaller scale (see Table 2 and Section 4.2). Batch A0-AN1-5 reached an average normalized area of 2.66 at 855 °C. Batches A0-AN1-45 and A0-AN1-75 produced moderate amounts of foam and behaved similarly to each other, as shown by overlapping error bars, with maximum normalized areas of 1.49 at 880 °C and 1.61 at 875 °C, respectively. As overlapping error bars indicate, batches A0-AN1-150 and A0-AN1-195 were even more similar to each other than were A0-AN1-45 and A0-AN1-75, with normalized areas of 1.11 and 1.05, respectively, at 900 °C (see Table 2).

3.3. A0-AC and A0-AN2

Fig. 5 shows A/A_g versus temperature for the A0-AC and A0-AN2 batches.

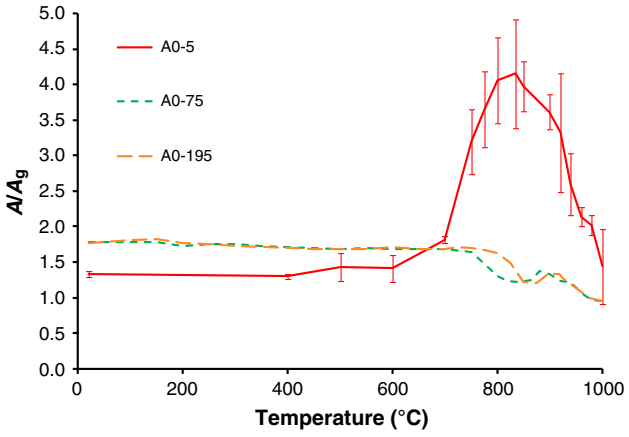

Fig. 3. Expansion of pellets made from A0 batches (the lines connect data points representing averaged values).

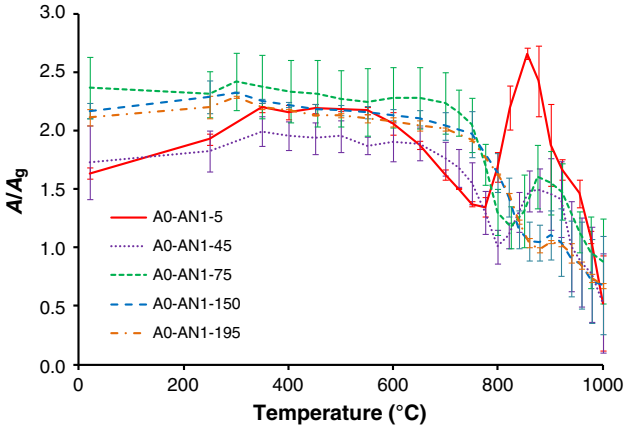

Fig. 4. Expansion of pellets made from A0-AN1 batches (the lines connect data points representing averaged values).

The carbonate batch, A0-AC, exhibited almost no foam, only reaching an average normalized area of 0.99 at 875 °C. The A0-AN2 batches exhibited two different foaming patterns, depending whether C/N<1 or ≥1. Batches with C/N<1 reached their minima at 825 °C with $A/A_g \approx 0.88$ and their maxima at 925 °C with $A/A_g \approx 1.4$. These expansion curves for these three batches are virtually indistinguishable from each other past 775 °C. Batches with C/N≥1 reached their minima at 800 °C with $A/A_g \approx 1.2$ and their maxima at 925 °C with $A/A_g \approx 2.0$ (see Table 2).

3.4. Volume expansion

Batches A0-AN2 (0.00), A0-AN2 (0.50), and A0-AN2 (0.75) expanded from a minimum normalized volume ≈1 to approximately 8 (Fig. 6) with gases comprising 87 vol% at 925 °C. Darab et al. reported expansion on a similar scale in a batch for a low-activity waste glass [11]. The normalized volume of A0-AN2 (1.00) grew from 1.5 to 11, while that of A0-AN2 (1.25) grew from 1.3 to 10. Both these melts contained 90 vol% gas phase at 925 °C.

4. Discussion

As seen in Figs. 4 and 5, for some batches at temperatures approaching 1000 °C, $A/A_g<1$, while $V/V_g \rightarrow 1$ as the glass became bubble free. This is expected because the cross-section area of a cylinder or a spherical cap with a constant volume varies as the ratio h/r changes, where h is the height, and r is the radius, for a cylinder, or

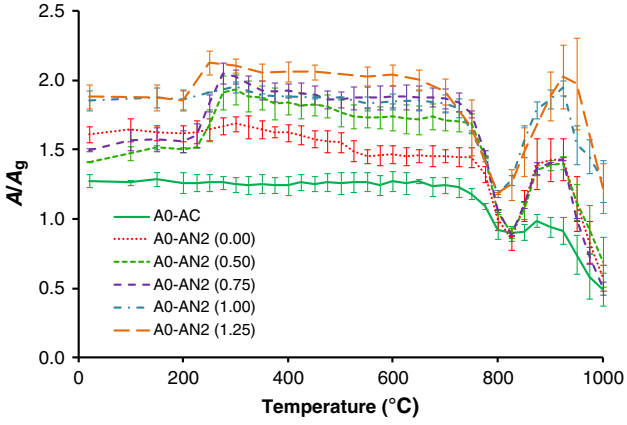

Fig. 5. Expansion of pellets made from A0-AC and A0-AN2 batches (the lines connect data points representing averaged values).

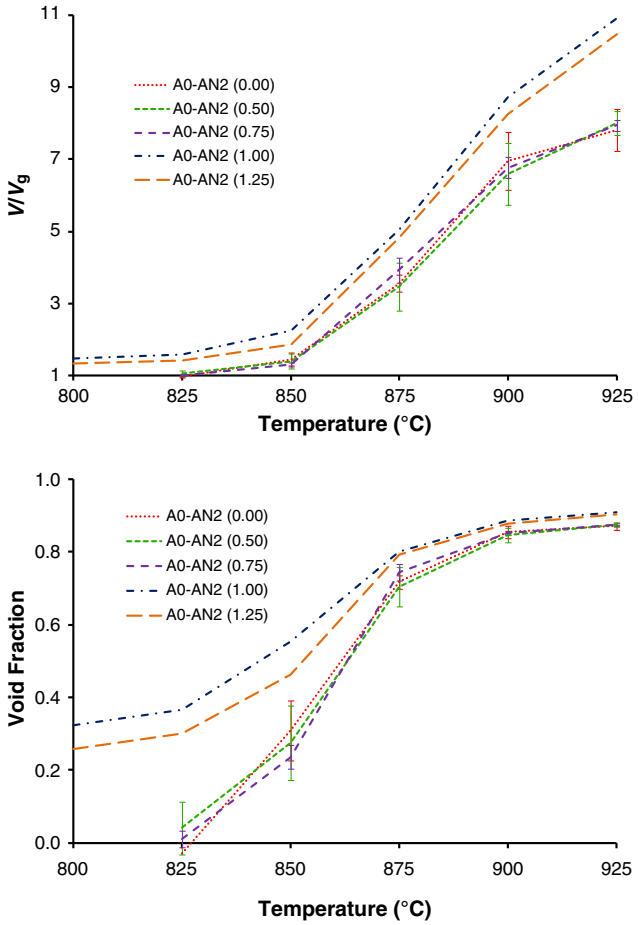

Fig. 6. Relative volume and void fraction versus temperature for pellets made from A0-AN2 batches (the lines connect data points representing averaged values).

half the width of the base for a spherical cap. For a cylinder, this relationship is expressed by

$$\frac{A}{V^{\frac{2}{3}}} = 2\pi^{-\frac{2}{3}} Z^{\frac{1}{3}} \tag{2}$$

where A is the cross-section area, V is the volume of glass, and $Z = h/r$.

For a spherical cap this relationship is expressed by

$$\frac{A}{V^{\frac{2}{3}}} = \left(\frac{4\pi}{3}\left(3+Z^2\right)\right)^{-\frac{2}{3}}\left[Z^{-\frac{8}{3}}\left(1+Z^2\right)^2 \cos^{-1}\left(\frac{1-Z^2}{1+Z^2}\right) - 2Z^{-\frac{5}{3}}\left(1-Z^2\right)\right] \tag{3}$$

where A is the cross-section area, V is the volume of glass, and $Z = h/r$.

Fig. 7 shows these relationships.

4.1. Primary and secondary foam

Two types of foam occur during batch melting: primary foam, the expansion of the batch by evolving batch gases trapped in the glass-forming melt, and secondary foam, an accumulation of fining bubbles from molten glass. In our previous study [6], a batch formulated to make a high-alumina glass with a composition similar to the A0 glass produced two peaks on its expansion curve, one for primary foam and one for secondary foam. This effect was not seen in the batches prepared for this study. For the A0-5 and A0-AN1 batches, instead of the primary foam subsiding before the secondary foam developed, the primary foam subsided after the secondary foam had begun to develop, producing a single peak. The batches with larger quartz

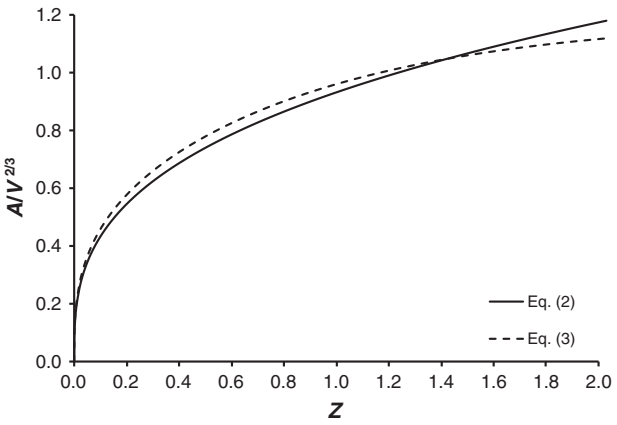

Fig. 7. Plot of Eqs. (2) and (3).

particles or sucrose formed no primary foam at all and only produced secondary foam.

Fig. 8 shows the correlation between the maximum profile area of a pellet and the temperature of the minimum area. Our data indicate that batches that reach their minimum expansion at a lower temperature tend to produce a larger amount of foam. This occurs because batches reach their minimum at the point when a continuous melt is established. The earlier this melt is established, the more foam-generating gases can be trapped. For example, the A0-5 batch begins to form a continuous melt at 600 °C and can then trap the gases that evolved from that point until the source of foam becomes depleted, and the viscosity becomes too low, and then the foam collapses. The sources of primary foam, i.e., batch reaction gases, are evolved up to only 800 °C [11]. This means that the A0-195 batch, which begins to connect at 875 °C, or any other batch that reaches its minimum at or later than 800 °C, cannot retain these gases and therefore cannot form foam. The trend in foaming for A0-AN2 along with the effect of sucrose addition is discussed in Sections 4.2 and 4.4.

4.2. Effect of silica size

As shown in previous studies, [4,6,7] the size of the quartz particles has a large effect on the rate of silica dissolution and on foaming. Very small quartz particles lead to large amounts of primary foam. This occurs because small quartz grains dissolve faster than larger grains, creating high concentrations of dissolved silica earlier than larger grains do. This early formation of a viscous continuous melt traps the gases from the final stages of the degradation of the nitrates and

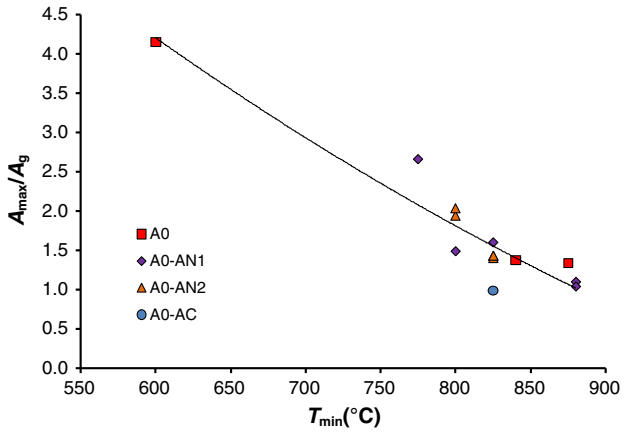

Fig. 8. Correlation between temperature of minimum expansion (T_{min}) and maximum normalized area (A_{max}/A_g) for all batches (a second-order polynomial was fitted to data to guide the eyes).

carbonates present in the batch. The degradation of nitrates, nitrites, and carbonates in the A0 batch, when totally completed, produces a volume of gas that would be 403 times larger than the volume of glass at $T = 925$ °C. For the other batches, these numbers are even larger: 936 in A0-AC, 2496 in A0-AN1, and 2567 in A0-AN2. Because only the end of this degradation is captured as foam, any delay in forming a continuous melt will result in a reduction in primary foam. As the quartz particle size increases, the silica resists dissolution. This leads to a later formation of a continuous melt and less primary foam. Large grains also tend to form agglomerates [4], which further hinders dissolution.

Secondary foam is less affected by the size of silica grains as it always forms after a continuous melt has been established. However, larger grains do reduce secondary foam as they dissolve slower, which contributes to a lower viscosity in the melt and a reduced ability to retain bubbles. The kinetics of quartz dissolution will be further investigated in the next paper in this series.

4.3. Differences between carbonates and nitrates

The A0-AC batch was included to see if there would be any difference in foam generation between a batch that contained no nitrates from the start and a batch that did contain nitrates, but that were removed by reaction with sucrose during the melting process. As Fig. 5 shows, there is a marked difference. The carbonate batch produced very little secondary foam in relation to other batches with 75-μm silica.

4.4. Effect of sucrose

The expansion around 200 to 400 °C in some batches (see Figs. 4 and 5) may be due to a tendency of sucrose to caramelize at ~170 °C and trap some of the early batch reaction gases. However, the lack of low-temperature expansion in the A0-AN2-75 (1.00) batch (Fig. 5) indicates that this effect is probably random.

The sucrose addition appears to decrease the amount of foam in nitrate-containing batches, though this effect is only seen with small silica grains (Fig. 9). As seen in Table 2 and Fig. 3, the A0-5 pellets had a maximum relative area of 4.15 at 835 °C, while the A0-AN1-5 pellets had a maximum relative area of 2.66 at 855 °C. This decrease in foam can be attributed to the reaction between sucrose and nitrates that occurs between 150 °C and 300 °C [6]. This early decomposition of nitrates caused less gas to be evolved at higher temperatures and reduced the formation of primary foam. This accounts for the large difference between A0-5 and A0-AN1-5 seen in Fig. 9. With larger quartz particles though, this effect is masked by the absent primary foam inherent with larger grains; compare A0-75 and A0-AN1-75, or A0-195 and A0-AN1-195 in Fig. 9.

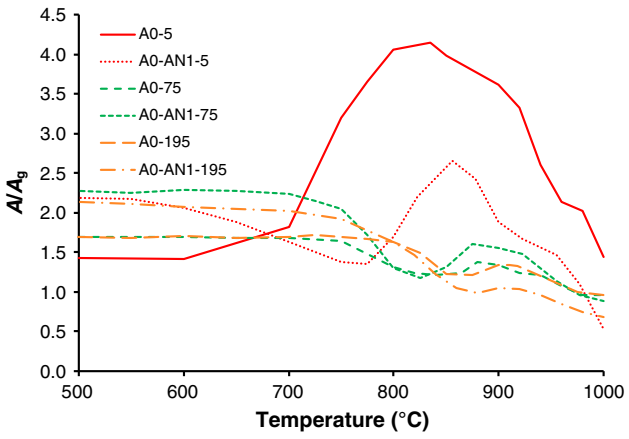

Fig. 9. Expansion of pellets made with A0 and A0-AN1 batches (the lines connect data points representing averaged values).

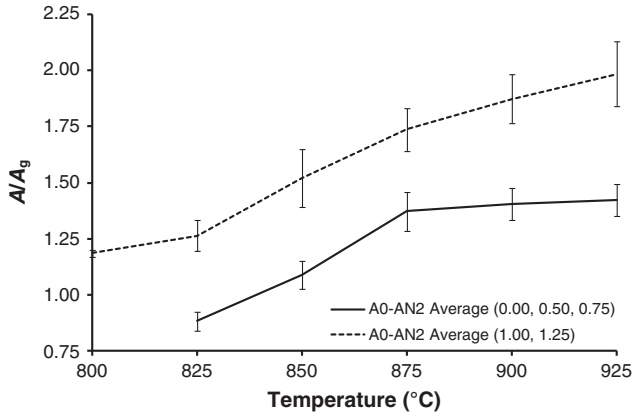

Fig. 10. Average of A0-AN2 (0.00), A0-AN2 (0.50), and A0-AN2 (0.75) expansions from 825 °C to 925 °C and the average of A0-AN2 (1.00) and A0-AN2 (1.25) expansions from 800 °C to 925 °C (the lines connect data points representing averaged values).

Sucrose does have an effect on secondary foam, however, as seen in A0-AN2 (Fig. 5) and described in Section 3.3. The amount of secondary foam does not increase with the amount of sucrose while C/N is between 0.00 and 0.75, but does increase when C/N ≥ 1. Fig. 10 illustrates the difference. This effect is not entirely unexpected, as will be explained in the following section.

4.5. Growth and collapse of secondary foam

The growth and collapse of secondary foam can be rationalized with the following scenario. The secondary foam is caused by the oxidation–reduction reactions that occur in the melt [12]. As long as nitrates are present, the O_2 given off by their decomposition is keeping the ferric–ferrous ratio high. Eventually all nitrates decompose and the melt shrinks to its minimum volume. At this point, there is a high concentration of dissolved oxygen and water in the melt. This water and oxygen then diffuse into small residual bubbles that began to grow, eventually expanding into foam. As the bubbles expand, the diffusion distances within the films of melt separating the bubbles shorten, and gases in the melt easily approach equilibrium with gases in bubbles. As the concentration of oxygen in the melt decreases, the reduction of Fe_2O_3 to FeO progresses, producing even more gas. This reduction is also fueled by the dissolution of hematite into the melt and the precipitation of magnetite [6]. Finally, the bubbles in the foam coalesce into larger and larger cavities while the viscosity of the glass decreases with the increasing temperature. After the bubbles burst out of the melt, a depleted supply of dissolved oxygen in conjunction with a less viscous melt leads to the collapse of the foam. The melt continues to evolve gas from oxidation–reduction reactions, but these reactions do not produce enough gas and the melt is no longer viscous enough to retain the evolving gas.

The expansion observed in A0-AN2 would require the reduction of 20 mass% of the Fe_2O_3 present in the melt. This greatly exceeds the 3 to 4 mass% of Fe_2O_3 that has been reported to react in HLW glasses [12]. The presence of water in foam was reported by Goldman [13]. If 1200 ppm of dissolved water (the concentration reported for soda-lime glass [14]) is released at 925 °C, the vapor volume per volume unit of glass could be as high as 17. The presence of water vapor in the foam could account for the difference between the observed volume and the volume of oxygen available from the reduction of Fe_2O_3.

In A0-AN2 (0.00), A0-AN2 (0.50), and A0-AN2 (0.75) batches, the amount of sucrose was insufficient for the total destruction of the nitrates, leaving all or some of the nitrates to decompose "naturally," allowing secondary foam to form as described above. This did not happen for A0-AN2 (1.00) or A0-AN2 (1.25), creating a different foaming behavior for these two batches.

This difference between those batches with C/N<1 and those with C/N≥1 can be seen already at the point at which the melt reached the minimum volume. As Fig. 6 shows, batches with C/N<1 reached their minimum volume at 825 °C with nearly zero porosity, whereas those with C/N≥1 reached their minimum volume at 800 °C with around 30% porosity. We can assume that nearly all nitrates reacted with sucrose at a low temperature in A0-AN2 (1.00) and A0-AN2 (1.25) batches, which would decrease the partial pressure of oxygen in the melt. The absence of any primary foam gases dissolved in the melt allowed the reduction of Fe_2O_3 to produce O_2 below 800 °C, thus initiating secondary foam earlier than in other batches. The possible presence of carbon from unreacted sucrose could also lead to the evolution of CO_x. In addition to contributing to secondary foam, the CO_x would, together with water, lower the partial pressure of oxygen in bubbles. However, the little difference in foam volume between batches with C/N=1 and C/N=1.25 suggests that the complete reaction of nitrates early in the melt causing an earlier closure of open pores and trapping more gases contributed more to secondary foam than excess carbon from sucrose.

It is questionable whether this effect operates in batches other than those with an intermediate silica size, i.e., 75 μm, and – as the similarity in foaming between 45-μm batches and 75-μm batches (Fig. 4) suggests – 45 μm as well. As seen in Fig. 9, adding sucrose diminished foam for batches with 5-μm quartz particles while having no effect on batches with larger particles.

4.6. Recommendations for large-scale melters

Primary foam hinders the transfer of heat to the cold cap from the molten glass and reduces the rate of melting. While secondary foam can be removed by bubbling air through the melt, primary foam remains within the cold cap and cannot be removed by mechanical means. Therefore, primary foam should be avoided if possible. The pellet test used in this study is a good tool for measuring the extent of primary and secondary foam and as such can be recommended as a screening test for selecting batch materials.

Since smaller sizes of quartz grains lead to increased primary foam and larger sizes dissolve too slowly and decrease melt homogeneity [4], medium-sized quartz grains (around 45–75 μm) may be recommended for achieving optimum performance from large-scale melters.

Sucrose is occasionally added to waste-glass batches containing nitrates to control oxidation–reduction reactions or to enhance the melt rate [15]. Our study indicates that sucrose can also help reduce primary foam in batches with nitrates, though additions of C/N≥1 could result in increased secondary foam. Moreover, it seems possible that grains of quartz even smaller than 45 μm may be used in combination with sucrose addition in batches with nitrates without worrying about the increased primary foam that usually results from using small quartz particles.

5. Conclusions

The batch reaches its minimum volume when the glass-forming melt becomes connected and open porosity closes. This minimum is immediately followed by the formation of foam. Residual batch gases generate primary foam, whereas gases that evolved from oxidation–reduction reactions generate secondary foam. The extent of the foam decreases as the size of quartz particles increases. The use of micrometer-sized quartz particles causes large volumes of primary foam because of the quick dissolution of the silica and the early formation of a connected melt. Batches containing larger quartz particles (≥45 μm) do not generate primary foam. A moderate addition of sucrose (up to C/N=1) has no impact on foaming except for batches with nitrates and micrometer-sized quartz particles, where it substantially decreases primary foam. Higher amounts of sucrose in nitrate-containing batches mildly increase secondary foam. The A0-AC batch, which contained carbonates and no nitrates, did not produce foam.

The rise in foaming after the porosity closes is quite rapid because the melt is oversaturated with oxygen that cannot easily diffuse out of the melt. As the melt turns to foam, the diffusion distances shorten and gas can be quickly released, turning the melt into very low density foam. The porosity of the foam at its maximum volume is about 90%. The foam collapses from within, forming large cavities that eventually burst into the atmosphere. The extent of foaming is inversely proportional to the temperature at which the batch volume reaches a minimum.

This study also shows that pellet tests are suitable for rapid measurement of batch volume as a function of temperature and batch makeup parameters. Obtaining volume measurements does require numerical integration of the pellet profile, however.

Acknowledgments

Pacific Northwest National Laboratory (PNNL) is operated for the U.S. Department of Energy by Battelle under Contract DE-AC05-76RL01830. The authors are grateful to the U.S. Department of Energy WTP Project Office Engineering Division for financial support and Albert Kruger for his assistance and guidance. The authors would like to thank Dong-Sang Kim for discussions about the waste-glass melting process and his meticulous review, and Carissa Humrickhouse for help in preparing batches as well as her initial work concerning the effect of C/N ratios in glass batches.

References

[1] P.R. Laimböck, Foaming of glass melts, University of Technology, Eindhoven, Ph.D. Thesis, 1998.
[2] A.G. Fedorov, L. Pilon, J. Non-Cryst. Solids 311 (2002) 154.
[3] H. Gerrard, I.H. Smith, Glastech Ber-Glass 56K (1983) 13.
[4] M.J. Schweiger, P. Hrma, C.J. Humrickhouse, J. Marcial, B.J. Riley, N.E. TeGrotenhuis, J. Non-Cryst. Solids 356 (2010) 1359.
[5] P. Hrma, M.J. Schweiger, C.J. Humrickhouse, J.A. Moody, R.M. Tate, N.E. TeGrotenhuis, B.M. Arrigoni, C.P. Rodriguez, Proc. Int. Symp. Rad. Saf. Manag. (2010) 280, Daejeon, Republic of Korea.
[6] P. Hrma, M.J. Schweiger, C.J. Humrickhouse, J.A. Moody, T.T. Tate, N.E. Rainsdon, B. M. TeGrotenhuis, J. Arrigoni, C.P. Marcial, B.H. Rodriguez, Tincher, Ceramics-Silikaty 54 (2010) 193.
[7] J. Marcial, P. Hrma, M.J. Schweiger, K.J. Swearingen, N.E. TeGrotenhuis, S.H. Henager, Proc. INMM 51st Annual Meeting, Baltimore, July 11-15, 2010, 2010.
[8] D.A. Pierce, P. Hrma, M.A. Steward, M.J. Schweiger, Proc. Mat. Sci. & Technol. 112th Annual Meeting, 2010.
[9] K.S. Matlack, H. Gan, M. Chaudhuri, W. Kot, W. Gong, T. Bardakci, I. Pegg, DM100 and DM1200 Melter Testing with High Waste Loading Glass Formulations for Hanford High-Aluminum HLW Streams, VSL-10R1690-1, Vitreous State Laboratory, Washington DC, 2010.
[10] R.L. Russell, J.M. Billing, R.A. Peterson, D.E. Rinehart, H.D. Smith, Development and demonstration of ultrafiltration simulants, PNNL-18090, Pacific Northwest National Laboratory, Richland, Washington, 2009.
[11] J.G. Darab, E.M. Meiers, P.A. Smith, Behavior of simulated Hanford slurries during conversion to glass, Mat. Res. Soc. Proc. 556 (1999) 215.
[12] P. Hrma, G.F. Piepel, M.J. Schweiger, D.E. Smith, D-S. Kim, P.E. Redgate, J.D. Vienna, C.A. LoPresti, D.B. Simpson, D.K. Peeler, and M.H. Langowski, *Property/Composition Relationships for Hanford High-Level Waste Glasses Melting at 1150°C*, PNL-10359, Vol. 1 and 2, Pacific Northwest Laboratory, Richland, Washington, 1994.
[13] D.S. Goldman, J. Non-Cryst. Solids 84 (1986) 292.
[14] F. Geotti-Bianchini, J.T. Brown, A.J. Faber, H. Hessenkemper, S. Kobayashi, I.H. Smith, Glastech. Ber-Glass Sci. Technol. 72 (1999) 145.
[15] J.E. Josephs, M.E. Stone, Melt Rate Improvement for DWPF MB3: Sugar Addition Test. WSRC-TR-2001-00158, Westinghouse Savannah River Company, Aiken, South Carolina, 2001.